Ultrafast electrocyclic ring opening of 7-dehydrocholesterol in solution: The influence of solvent on excited state dynamics

Kuo-Chun Tang, Aaron Rury, Michael B. Orozco, Joshua Egendorf, Kenneth G. Spears et al.

Citation: J. Chem. Phys. **134**, 104503 (2011); doi: 10.1063/1.3557054
View online: http://dx.doi.org/10.1063/1.3557054
View Table of Contents: http://jcp.aip.org/resource/1/JCPSA6/v134/i10
Published by the AIP Publishing LLC.

Ultrafast electrocyclic ring opening of 7-dehydrocholesterol in solution: The influence of solvent on excited state dynamics

Kuo-Chun Tang, Aaron Rury, Michael B. Orozco, Joshua Egendorf, Kenneth G. Spears, and Roseanne J. Sension[a)]
Department of Chemistry and Department of Physics, University of Michigan, 930 N. University Ave., Ann Arbor, Michigan 48109-1055, USA

(Received 2 December 2010; accepted 1 February 2011; published online 10 March 2011)

Broadband UV-visible femtosecond transient absorption spectroscopy and steady-state integrated fluorescence were used to study the excited state dynamics of 7-dehydrocholesterol (provitamin D_3, DHC) in solution following excitation at 266 nm. The major results from these experiments are: (1) The excited state absorption spectrum is broad and structureless spanning the visible from 400 to 800 nm. (2) The state responsible for the excited state absorption is the initially excited state. Fluorescence from this state has a quantum yield of $\sim 2.5 \times 10^{-4}$ in room temperature solution. (3) The decay of the excited state absorption is biexponential, with a fast component of ~0.4–0.65 ps and a slow component 1.0–1.8 ps depending on the solvent. The spectral profiles of the two components are similar, with the fast component redshifted with respect to the slow component. The relative amplitudes of the fast and slow components are influenced by the solvent. These data are discussed in the context of sequential and parallel models for the excited state internal conversion from the optically excited 1^1B state. Although both models are possible, the more likely explanation is fast bifurcation between two excited state geometries leading to parallel decay channels. The relative yield of each conformation is dependent on details of the potential energy surface. Models for the temperature dependence of the excited state decay yield an intrinsic activation barrier of ~2 kJ/mol for internal conversion and ring opening. This model for the excited state behavior of DHC suggests new experiments to further understand the photochemistry and perhaps control the excited state pathways with optical pulse shaping. © *2011 American Institute of Physics*. [doi:10.1063/1.3557054]

I. INTRODUCTION

Photochemical isomerization reactions of simple polyene chromophores play a key role in the function of many important biological systems.[1,2] Typical examples include the *cis–trans* isomerization reactions of retinal in rhodopsins and of the chromophore in photoactive yellow protein[1–3] as well as the electrocyclic ring-opening reaction of 7-dehydrocholesterol (provitamin D_3, DHC).[4–7] There has been much interest over the last several years in the potential for optical control of these polyene chromophores, both in natural biological systems and in synthetic constructs designed to operate as light activated switches.[8–17] Any attempt to control and optimize photochemical isomerization reactions of polyene chromophores must include an understanding of details specific to individual chromophores, general trends in molecular properties, the role played by competing reactions, and the influence of environment on molecular dynamics. In the work reported here we present the results of femtosecond transient absorption experiments designed to explore the excited electronic state properties of DHC and the influence of the solvent environment on the excited state dynamics.

DHC is a complex molecule that plays an important role as precursor in the natural production of vitamin D_3.[18,19] The photochemical scheme for the formation of vitamin D_3 involves UV excitation of a 1,3-cyclohexadiene chromophore embedded in the much larger molecule (Fig. 1). Excitation of the cyclohexadiene chromophore results in electrocyclic ring opening to form a conjugated triene species which undergoes a thermal hydrogen migration to form vitamin D_3. The photochemistry of DHC and production of vitamin D_3 is complicated by a web of photochemical pathways and byproducts.[19,20] Most of these byproducts are conjugated dienes or trienes that absorb in the UV between 300 and 250 nm. Thus the desired yields and photostationary states are wavelength dependent.[6,20–23] In addition the solvent environment plays a significant role in the conformational equilibrium of previtamin D_3 and on the various photochemical pathways.[24,25]

The electronic absorption spectrum of DHC is located in the UV, with the lowest allowed transition peaking at 282 nm (see Fig. 2). Compared with the corresponding transition in the isolated 1,3-cyclohexadiene molecule (CHD), the spectrum is redshifted, stronger, slightly narrower and more structured. The DHC spectrum exhibits a vibrational progression of $\sim 1350\ cm^{-1}$ with at least four and as many as six bands visible in the progression. This mode is consistent with a displacement along delocalized C=C stretching coordinates in the excited state, typical of $\pi \rightarrow \pi^*$ transitions in conjugated polyenes. A much less prominent vibrational progression can be seen in the CHD spectrum.[26] The DHC spectrum measured in alcohols (methanol, ethanol, n-propanol, and 2-butanol) and alkanes (heptane, dodecane, and hexadecane)

a)Electronic mail: rsension@umich.edu.

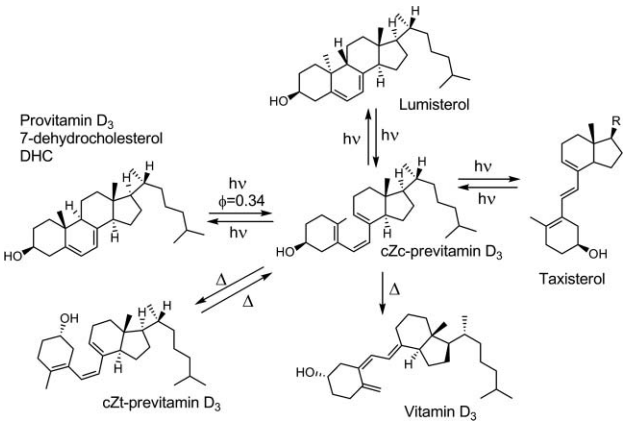

FIG. 1. The provitamin D_3 7-dehydrocholesterol (DHC) molecule undergoes a photochemical ring-opening reaction to form cZc-previtamin D_3 which undergoes conformational relaxation producing an equilibrium mixture of the cZc and cZt conformers. The cZc-previtamin D_3 undergoes a hydrogen transfer and electronic rearrangement to form vitamin D_3. Photochemical side reactions compete with formation of vitamin D_3. The hydrocarbon tail, R, on taxisterol is the same as for the other compounds.

is weakly dependent on the solvent, with peak shifts of under 0.4 nm and slight differences in band width. The maximum extinction coefficient (ε_{max}) is $\sim 1 \times 10^4$ M^{-1} cm^{-1}, approximately a factor of two larger than ε_{max} for cyclohexadiene ($\sim 5 \times 10^3$ M^{-1} cm^{-1}).

Early UV transient absorption measurements of both CHD (Refs. 27–31) and DHC (Refs. 4–7) concentrated on the photoproduct formation and conformational relaxation. Studies of DHC in methanol, ethanol, and heptane solvents demonstrated the rapid internal conversion from the excited state manifold and formation of vibrationally and conformationally excited molecules on a picosecond time scale.[4–7] Product formation is followed by vibrational relaxation on a time scale of 2–9 picoseconds in heptane and 2–5 ps in methanol.[4,5] Conformational relaxation leading to an equilibrium mixture of cZt and cZc conformers occurs on a time scale >100 ps in heptane and ~100 ps in methanol. Temperature dependent measurements by Fuss *et al.*[7] determined the ground state barrier for conformational relaxation for the cZc → cZt-previtamin D transition to be $\sim 15.5 \pm 1$ kJ/mol in methanol and ethanol solvents.

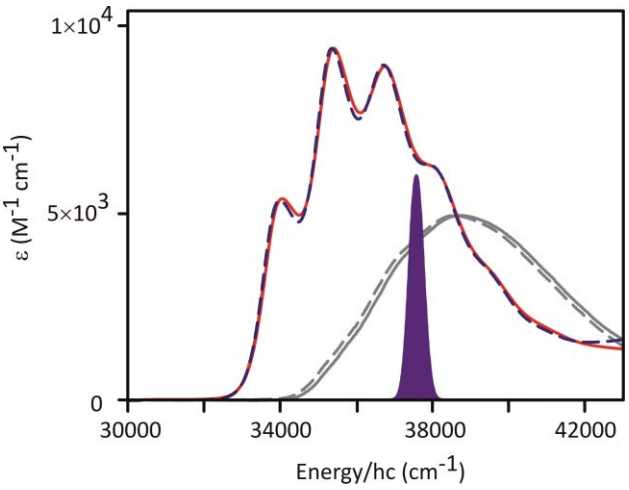

FIG. 2. Absorption spectrum of 7-dehydrocholesterol (DHC) in hexadecane (blue dashed line) and methanol (red line). The absorption spectra of 1,3-cyclohexadiene in methanol and hexadecane are indicated in gray for comparison. The excitation pulse is 3 nm wide, centered at 266.3 nm. This is also indicated in the figure. The extinction coefficients are accurate to two significant figures.

Direct observation of the excited state dynamics involved in the ring-opening reaction in DHC and CHD has proven somewhat elusive. There is no clean signature of the excited state of CHD in solution. However, extensive studies in the gas phase using multiphoton ionization to detect and differentiate excited state species have provided detailed information on the motions inherent in the excited state ring-opening reaction.[26,32–34] A recent study by Kosma *et al.*[26] using ultrashort 13 fs UV excitation pulses identified time constants for motion along the excited state surfaces and followed coherent vibrational motion on the excited state surface. This work demonstrates that the ring opening begins on the initially excited 1^1B surface, continues on the dark 2^1A state, and is completed following internal conversion to the ground state surface. The initially prepared excited state population decays in ~21 fs accompanied by C=C bond elongation and twisting, internal conversion to the dark state occurs in ~35 fs accompanied by stretching of the C–C bond. The decay of the 2^1A state is ~80 fs accompanied by a much larger distortion from the near planarity of the initial chromophore. The reaction is described as "more or less ballistic" with negligible barriers along the reaction path.

Unlike CHD, a strong visible excited state absorption signal is observed following excitation of DHC.[4,5] Transient absorption experiments revealed a ~1 ps decay, weakly dependent on the solvent. The excited states of both DHC and the related ergosterol (provitamin D_2) chromophore were also detected via fluorescence in low temperature organic matrices.[19,35] At 77 K in a methylcyclohexane–isopropane matrix both ergosterol and DHC are fluorescent,[35] although only the spectrum of ergosterol is shown in Ref. 35. The spectrum of ergosterol is a good mirror image of the absorption spectrum with no significant Stokes shift.[19,35] The fluorescence lifetime, τ_f, is 3.3 ns, and the fluorescence quantum yield, ϕ_f, is 0.19.[35] Similar lifetimes were measured by Nakashima *et al.* in other matrices at 77 K. The radiative lifetime of $\tau_r = \tau_f/\phi_f = 17.4$ ns measured in these experiments is significantly longer than the intrinsic lifetime of 4.25 ns they calculated from the absorption spectrum.[35,36] The temperature dependence of the fluorescence intensity between 89 and 150 K predicts an activation energy for nonradiative decay of 11.1 ± 0.15 kJ/mol with an Arrhenius prefactor of 40 ± 20 ps^{-1}. Because no fluorescence was observed at low temperature in a supersonic jet ($\phi_f < 0.005$) the activation energy was assigned to the solvent activation energy rather than an intrinsic intramolecular barrier.

The ability to directly probe the excited state dynamics of DHC in room temperature solution through a strong visible excited state absorption suggests interesting possibilities for elucidation of the excited state dynamics, the nature of the excited states responsible for the reaction, and for optical control of the ring-opening process itself. The earlier transient absorption studies however, were performed at specific isolated

wavelengths with relatively low signal to noise.[4,5] These measurements provide only a sketch of the excited state dynamics. In the work described here we report studies to characterize the excited state(s) of DHC observed following excitation at ~266 nm. Steady state fluorescence is used to identify the excited state while broadband transient absorption spectroscopy is used to characterize the excited state dynamics. The absorption probe spans the entire visible region of the spectrum from 340 to 800 nm. These studies use the spectral profile, solvent dependence and temperature dependence to explore the excited state of the DHC chromophore.

II. EXPERIMENTAL

Femtosecond pump-probe transient absorption measurements were performed using two different laser systems. For the first set of experiments a femtosecond Ti:sapphire oscillator seeded a home-built 1 kHz multipass ultrafast amplifier to generate femtosecond laser pulses with a central wavelength of 797 nm, pulse duration of ~60 fs and pulse energy of ~700 μJ. A beamsplitter was used to generate pump and probe pulses separately. The major portion (650 μJ) was frequency-doubled and then frequency-summed with residual fundamental to generate an ultraviolet femtosecond pulse with pulse energy of ~17 μJ at 266 nm. This UV pulse is temporally recompressed by passing through an acousto-optic programmable dispersive filter (AOPDF, Dazzler, Fastlite) to output a transform-limited UV pump pulse. The UV pulse centered at 266.3 nm puts ~3500 cm^{-1} of excess vibrational energy into the DHC molecule, including ~2 quanta of excitation in the Franck–Condon active 1350 cm^{-1} mode as illustrated in Fig. 2.

The minor portion of the fundamental beam (50 μJ) was delayed by a computer controlled optical delay line with respect to the pump and then focused into a 1 mm quartz flow cell containing ethylene glycol to produce a broadband white-light continuum pulse (400–780 nm). For some experiments white-light continuum was generated in a CaF_2 window; this extended the available spectrum, spanning the range from 340 to 800 nm.

Pump and probe pulses were both focused and overlapped with an angle of ~11° in an 0.5 mm quartz flow cell containing the DHC sample solution. Data were also obtained using a wire-guided free flowing stream of the DHC sample solution to avoid the influence of the cell wall on the pulse duration and the transient absorption signal. The beam diameter of the pump in the sample cell was about 140 μm measured by a knife-edge scan. DHC samples were excited with pump pulse energy of ~0.26 μJ. A mechanical optical chopper (MC1000A, THORLabs) was used to modulate pump pulses. The probe spectrum with pump on and pump off was recorded at each time delay point with a multichannel spectrometer (AvaSpec-2048-USB2, Avantes) and used to calculate the difference spectrum.

For most of the measurements the relative polarizations of the pump and probe pulses were set at magic angle (54.7°). An anisotropy measurement was also performed for DHC in 2-butanol and in heptane. The anisotropy was obtained by alternating parallel and perpendicular polarization of the pump beam with respect to the probe beam.

The temperature dependence of the excited state dynamics was measured using a second similar laser system. A home-built 1 kHz multipass ultrafast amplifier seeded by a Ti:Sapphire oscillator generated femtosecond laser pulses with central wavelength of 805 nm, pulse duration of ~60 fs and pulse energy of ~450 μJ. The pump was generated from the third harmonic of the laser and used without additional compression. The probe pulse was generated using a home-built noncollinear optical parametric amplifier tunable from 470 to 700 nm. Measurements were performed with the relative polarizations of the pump and probe pulses set at the magic angle of 54.7°. Temperature control was achieved by immersing the sample reservoir in a bath consisting of a 50/50 mixture of water and ethylene glycol. The temperature of the bath was controlled by a Neslab RTE-111 Refrigerated Bath/Circulator, capable of maintaining temperatures from −25 to +150 °C. The samples were flowed through a 1 mm path length cell to refresh the sample volume between laser pulses, and the sample temperature was measured with a temperature probe inserted in a Y-joint located immediately after the sample cell. The temperature of the sample was varied from 1 to 97 °C and was maintained within ±0.5 °C. The exact temperature range used for the experiment varied depending on the melting and boiling points of the solvent.

The fluorescence of DHC was measured at room temperature in heptane and 2-butanol by using a SPEX 500M spectrometer equipped with a 300 groove/mm grating and Princeton Instruments CCD camera. The fluorescence of *trans*-stilbene was used as a standard to calibrate both the spectral response of the spectrometer and the absolute quantum yield of the emission.

The 7-dehydrocholesterol sample was purchased from Aldrich and used without further purification. Sample concentrations were ~2.7 mM.

III. RESULT

A. Excited state spectrum

Typical time-resolved difference spectra obtained following the excitation of DHC in n-heptane and 2-butanol are shown in Fig. 3. The excited state spectrum exhibits a strong absorption peak at ~485 nm with a long tail extending to the red beyond 770 nm. The decay of the excited state absorption is consistent with earlier measurements of ~0.8 ps in heptane and 1.3 ps in 2-butanol.[4] Similar spectra were measured in methanol, ethanol, n-propanol, dodecane, and hexadecane. The spectral profile is slightly dependent on solvent and appears to contain contributions from transitions from the excited state populated by the excitation pulse, S_{exc}, to at least two different higher-lying excited states S_n.[37]

B. Anisotropy of the excited state absorption

The polarization anisotropy of the transient absorption was determined for DHC in heptane and 2-butanol

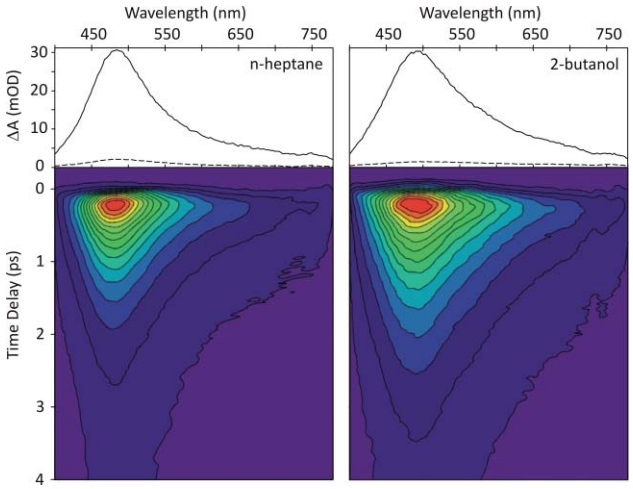

FIG. 3. Time-resolved "magic angle" difference spectra obtained following the excitation of DHC in n-heptane or 2-butanol at ~29 °C. The color scale ranges from maximum absorption (red) to no change in absorbance (purple). The traces at the top show the spectra due to excited state absorption of DHC at the peak of the transient signal (solid lines) and the persistent signal due to two photon ionization of the solvent (dashed lines). Similar spectra were obtained for DHC in methanol, ethanol, n-propanol, dodecane, and hexadecane solvents.

by measuring the spectrum for parallel and perpendicular polarizations of the pump pulse with respect to the probe pulse. This allows determination of both the average angle between the pumped and probed transition dipoles and the overall decay of the excited state absorption.[38] The population dynamics are obtained by constructing the magic angle trace as

$$I_{MA}(t) = \tfrac{1}{3}(I_{par} + 2I_{perp}), \quad (1)$$

where I_{par} and I_{perp} are the measured signals for parallel and perpendicular polarization of the pump pulse with respect to the probe pulse. The anisotropy is calculated as

$$r = \frac{I_{par} - I_{perp}}{I_{par} + 2I_{perp}} = \frac{2}{5}\langle P_2(\cos\theta)\rangle, \quad (2)$$

where $P_2[\cos(\theta)]$ is the second Legendre Polynomial $[P_2(x) = 0.5(3x^2 - 1)]$ of the cosine of the angle between the pumped and probed transition dipole moments. The brackets indicate an ensemble average. The anisotropy of the excited state absorption is highest near the peak of the absorption and significantly lower on the red side of the spectrum.[37] Decay traces and anisotropies for a selection of wavelengths spanning the observed spectral window are shown in Fig. 4. Except at early times on the blue edge of the spectrum, where two-photon absorption by the solvent contributes to the signal, the anisotropy is constant over the entire time window shown. The average angle between the pumped and probed transition dipole does not change with time. This is expected for a molecule the size of DHC if the nature of the transition $S_{exc} \rightarrow S_n$ responsible for the excited state absorption does not change, because the reorientational diffusion will be much slower than the picosecond lifetime of the excited state.

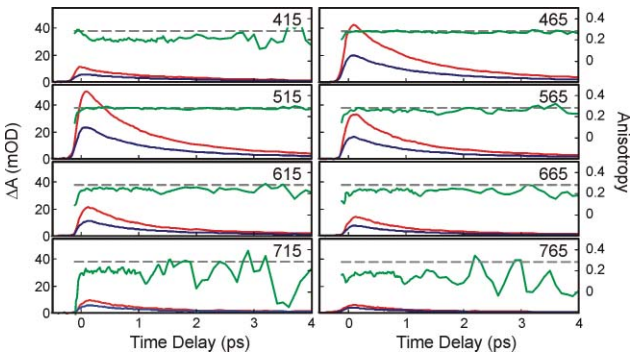

FIG. 4. Anisotropy decay following excitation of DHC in 2-butanol. Parallel (red) and perpendicular (blue) traces extracted from the spectral evolution at a selection of wavelengths spanning the observed spectral window. The anisotropy calculated from the individual traces is plotted in green. The gray dashed line represents the peak anisotropy of 0.28 for ease of comparison. The data were obtained at ~30 °C.

C. Steady state fluorescence

The fluorescence observed for ergosterol and DHC at low temperature suggests that fluorescence may also be observed for DHC in room temperature solution. In order to test this hypothesis and estimate the fluorescence quantum yield the integrated steady state fluorescence of *trans*-stilbene and DHC was measured in n-heptane and in 2-butanol. A control measurement using pure solvent resulted in no significant emission. The fluorescence observed for DHC in heptane is plotted in Fig. 5. This fluorescence is 2.5–3 orders of magnitude weaker than the fluorescence from *trans*-stilbene under the same conditions.

The fluorescence of *trans*-stilbene has been studied extensively as a function of both solvent and temperature. In n-heptane at 294.5 K the excited state lifetime is reported to be 85 ps (Refs. 39 and 40) and the rotational correlation time

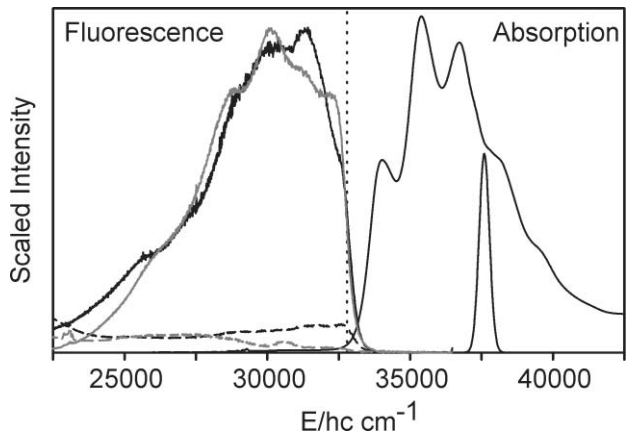

FIG. 5. Absorption and fluorescence spectra of DHC in n-heptane. The absorption spectrum and pump pulse (3 nm Gaussian centered at 266 nm) are plotted on the right side of the figure. The fluorescence spectra shown on the left are for two independent measurements. Both have been corrected for instrument response and background. The dashed lines represent the solvent background corrected for instrument response. The structure in the DHC fluorescence is not reproducible, but the overall shape is reproducible. The experimental setup had a sharp cutoff in detection efficiency at 305 nm (vertical dotted line) thus the emission spectrum of DHC may extend to somewhat higher energies.

is 19 ps.[41] Our transient absorption measurements yielded an excited state lifetime of 84 ± 9 ps and an anisotropy decay of 18 ± 2 ps in good agreement with the literature value. The fluorescence quantum yield for *trans*-stilbene in hexane is 4.33×10^{-2} at 299.8 K.[42] The quantum yield in heptane will be slightly higher. Based on a radiative rate constant of 6.0×10^{8} s^{-1} a quantum yield of 5.0×10^{-2} is a good estimate.[39] Using this value for *trans*-stilbene as a standard, the fluorescence quantum yield for DHC in heptane is $(2 \pm 1) \times 10^{-4}$.

The radiative lifetime of DHC in heptane is estimated at 5.8 ns using the Strickler–Berg equation[43] and approximating the index of refraction n with n_D:

$$\frac{1}{\tau_R} = k_r \approx \frac{8\pi n^2 2303}{N_A c^2} \langle \nu_f^3 \rangle \int \frac{\varepsilon(\nu_a)}{\nu_a} d\nu_a. \quad (3)$$

The measured quantum yield and estimated radiative lifetime permits an estimate of the excited state lifetime. The predicted excited state lifetime of DHC is $\phi_f/k_r = 1.2 \pm 0.6$ ps, slightly longer than the observed decay of ~0.8 ps.[4]

The DHC fluorescence was also measured in 2-butanol. The integrated fluorescence of DHC in 2-butanol is a factor of 9×10^{-3} weaker than the integrated fluorescence from *trans*-stilbene. The *trans*-stilbene excited state lifetime is 55 ± 5 ps. Assuming a radiative decay rate constant of 6.0×10^{8} s^{-1} the fluorescence quantum yield is 3.3×10^{-2}. Comparing the fluorescence yield from DHC and *trans*-stilbene in 2-butanol, the fluorescence quantum yield for DHC is $(3 \pm 1) \times 10^{-4}$. The estimated excited state lifetime is 1.7 ± 0.6 ps, again slightly longer than the observed 1.2 ps decay of the excited state absorption.[4]

The fluorescence anisotropy of DHC was determined by measuring the integrated fluorescence signal polarized parallel and perpendicular to the excitation laser. The laser polarization was rotated with a half-wave plate while the collection polarization remained constant. Measurements of the fluorescence anisotropy of *trans*-stilbene in heptane were used to confirm the accuracy of the measurement. Three measurements of the fluorescence anisotropy of DHC in heptane yielded values of 0.14, 0.12, and 0.12. In 2-butanol a value of 0.13 ± 0.01 was measured. Rotational reorientation is negligible during the short lifetime of the excited state in both heptane and 2-butanol (see Fig. 4). Thus the observed fluorescence anisotropy represents a rotation in the angle of the emissive dipole with respect to the absorptive dipole within the molecule. The average angle between the two transition dipoles is calculated to be $42^{o} \pm 1^{o}$ using the expression in Eq. (2).

The fluorescence quantum yield and the fluorescence spectrum suggest that the initially excited state of DHC is responsible for the excited state absorption. The similarity of the excited state lifetime and the inferred lifetime from fluorescence suggests no fast internal conversion to a 2^1A state as observed for CHD and other polyenes. There is an evidence for a fast rotation of the transition dipole, reflected in the low fluorescence anisotropy. The constant anisotropy measured in transient absorption (Fig. 4) suggests that the reorientation of the transition dipole occurs within 100 fs of excitation. Further implications of the low anisotropy will be considered below.

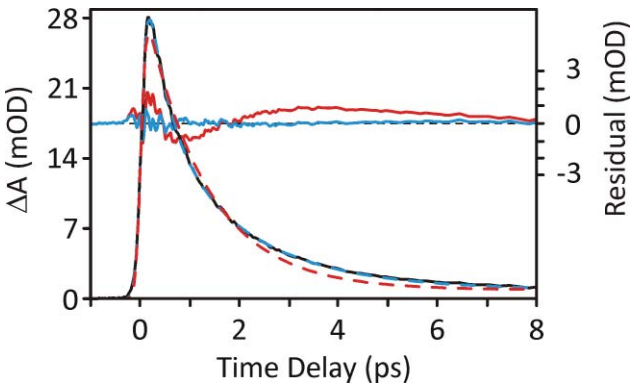

FIG. 6. Transient decay at 480 nm in 2-butanol (black). Both single exponential (red dashed) and biexponential (blue dashed) fits to the DHC ESA are shown along with the corresponding residuals (solid red and blue lines). Similar deviations between biexponential and single exponential fits are observed in all solvents at most wavelengths.

D. Excited state dynamics

The excited state dynamics in DHC were characterized by analyzing the transient absorption data every 10 nm across the spectrum. The kinetic traces were fit to a single exponential or biexponential decay of the excited state absorption convoluted with the instrument response modeled as a Gaussian. A small amplitude persistent signal attributed to solvent excitation was fit to a nondecaying amplitude. This signal is seen when the solvent alone is in the sample cell.[37] The parameters corresponding to the best fit to the data were determined using a simplex searching algorithm or a Levenberg–Marquardt algorithm to minimize the least-square deviation between the data and the fit. Comparisons of the experimental data with single and biexponential fits are plotted in Fig. 6 for $\lambda_{probe} = 480$ nm in 2-butanol. At very early times the data contain contributions attributed to two photon absorption and cross phase modulation.[44,45] The cross phase modulation is prominent in data obtained in a flow cell and minimal when the wire-guided flow was used.

The time constants obtained in single exponential fits are consistent with those reported earlier.[4,5] In general, however, a biexponential decay of the excited state is required by the much lower noise level in the present measurements. The residual for a single exponential decay shows substantial systematic deviation from zero as illustrated in Fig. 6. The intrinsic pulse width of ~90 fs prevents the excitation of high frequency vibrations. There is some evidence for a small oscillatory component in the signal obtained using the wire-guided flow sample (Fig. 6). This will warrant further investigation but is not the subject of this paper. Although it is impossible to rule out a nonexponential or multiexponential decay of the excited state absorption, and there is no reason to expect a perfectly exponential decay, the quality of the data does not warrant inclusion of additional components.

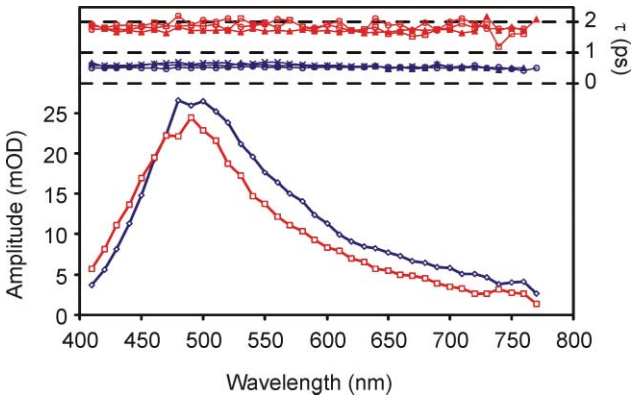

FIG. 7. Amplitude as a function of wavelength for the two exponential components contributing to the excited state decay of DHC in 2-butanol. Red: Amplitude and time constant for the slow component, 1.81 ± 0.15 ps. Blue: Amplitude and time constant for the fast component, 0.56 ± 0.06 ps. Time constants are plotted for three separate data sets. For clarity only the average amplitude is plotted.

1. Alcohols

A biexponential decay of the excited state absorption was required at all wavelengths in 2-butanol. The lifetime of DHC as a function of wavelength and the amplitudes of the two components are shown in Fig. 7. Data are shown for three different runs obtained on different days separated by several months. In every case the data are well modeled by a fast decay of 0.56 ± 0.06 ps and a slow decay of 1.81 ± 0.15 ps. The same decay constants are extracted from data sets obtained using a flow cell and data obtained with a wire-guided flow.

Similar biexponential decays were observed in methanol, ethanol, and 1-propanol solvents. These data are summarized in Fig. 8. The lifetime of the fast component is at most weakly dependent on the solvent. The lifetime of the slow time component exhibits a clear increase as the response time of the solvent slows from 1.06 ps in methanol to 1.8 ps in 2-butanol. The mechanism for the influence of solvent on the reaction dynamics is not clear from these data alone and will be discussed in more detail below. The spectral profiles of the fast and slow components are essentially independent of the solvent with the fast component redshifted 13 ± 2 nm with respect to the slow component. The amplitudes of the fast and slow components are dependent on the solvent as illustrated in Figs. 7 and 8.

2. Alkanes

Transient absorption spectra were also obtained for DHC in n-heptane, n-dodecane, and n-hexadecane solvents. Again the data are not well fit with a single exponential decay of the DHC excited state and require modeling with at least a biexponential decay of the ESA (Fig. 9). The deviation from a single exponential decay is smallest in heptane solvent, while dodecane and hexadecane exhibit deviations similar to those observed in the alcohols. In heptane the decay of the fast component is 0.65 ± 0.06 ps and the decay of the slow component is 1.39 ± 0.15 ps.

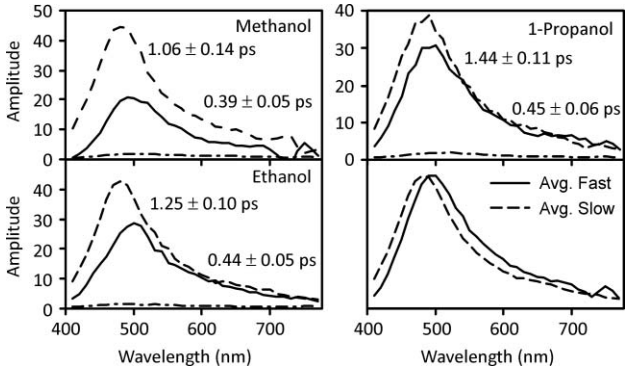

FIG. 8. Amplitudes for the fast (solid lines), slow (dashed lines), and long-lived solvent signals (dotted-dashed lines) as a function of wavelength in alcohol solvents. The bottom right hand panel compares the average spectral profile of the fast and slow components normalized to the same peak intensity.

In dodecane and hexadecane there are significant contributions arising from multiphoton ionization of the solvent. The solvent signals are still <10% of the peak intensity of the DHC ESA, nonetheless, this is sufficient to complicate the modeling of the decay dynamics attributed to DHC and leads to larger error estimates for the fits. In both hexadecane and dodecane the lifetime of the fast component is 0.55 ± 0.20 ps. The lifetime of the slow component is 1.25 ± 0.2 ps in dodecane and 1.4 ± 0.2 ps hexadecane. Within the error of the measurements the decay constants are independent of solvent properties from heptane to hexadecane.

The relative intensities of the two components depend on solvent. In hexadecane and dodecane the two components are of approximately equal amplitude, while in heptane the fast component clearly dominates with the slow component having ~35% the amplitude of the fast component. As for the alcohols, the spectral profiles of the fast and slow components in the alkanes are essentially identical for all three solvents. The fast component is redshifted ~4 nm and is somewhat narrower than the slow component as illustrated in Fig. 9(c).

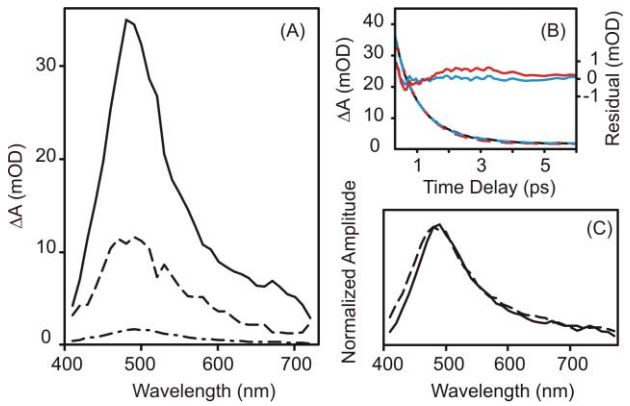

FIG. 9. (a) Amplitudes for the fast (solid lines), slow (dashed lines), and long-lived solvent signals (dotted-dashed lines) as a function of wavelength in n-heptane. (b) Comparison of the single exponential (red) and biexponential (light blue) fits to the experimental data at 480 nm (black) starting at 0.3 ps. The residuals plotted on the right axis are smaller than for the 2-butanol data (Fig. 6), but there is still a substantial systematic error for a single exponential fit (red). (c) Comparison of the average slow (dashed) and fast (solid) amplitudes in the three alkane solvents normalized to the same peak intensity.

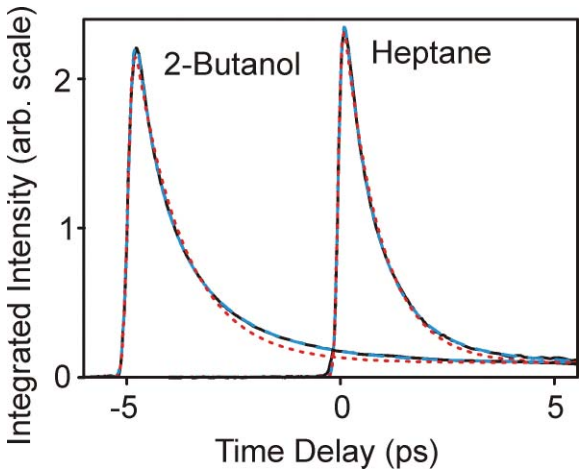

FIG. 10. Single exponential (red dotted lines) and biexponential (blue dashed lines) fits to the decay of the total integrated excited state absorption (black lines) of DHC in heptane and 2-butanol. The data in 2-butanol is offset by 5 ps for clarity.

3. Total integrated excited state absorption

The spectral shift observed for the fast and slow components in Figs. 8 and 9 suggests that the biexponential decay of the ESA may be due, at least in part, to relaxation of DHC in the excited state. Vibrational relaxation, conformational relaxation, and solvent relaxation could all contribute to the time dependence of the ESA. In most cases such spectral relaxation will conserve the total oscillator strength of the excited state absorption. In order to investigate the population dynamics separate from excited state relaxation, the excited state spectrum was integrated over the entire window for three independent measurements of DHC in 2-butanol and five independent measurements of DHC in heptane (Fig. 10). In 2-butanol the decay of the total integrated intensity is biexponential with time constants of 0.56 ps (56%) and 1.89 ps (44%). In heptane the integrated intensity decays with time constants of 0.61 ps (66%) and 1.32 ps (34%). The time constants and amplitudes are consistent with those obtained for individual wavelengths across the spectrum. While relaxation may contribute to the dynamics, it is not the major component. There is a biexponential decay of the total excited state population responsible for the absorption intensity.

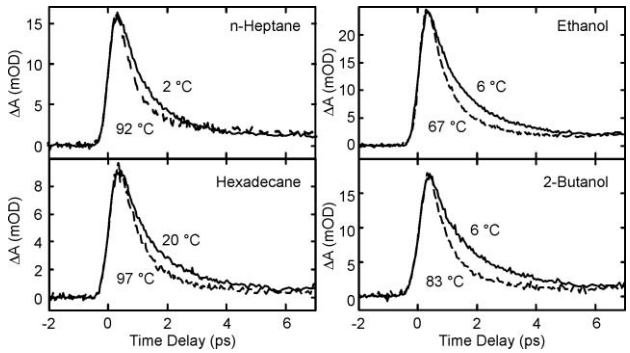

FIG. 11. Typical decay traces at the extremes of the temperature range in each solvent. The probe wavelength is 480 nm in 2-butanol and 500 nm in the other solvents.

TABLE I. Time constants for the biexponential fit to the decay of the transient absorption as a function of solvent. All measurements were made for temperatures between 26 and 29 °C.

Solvent	τ_1(ps)	τ_2(ps)
Methanol	0.39 ± 0.05	1.06 ± 0.14
Ethanol	0.44 ± 0.05	1.25 ± 0.10
1-Propanol	0.45 ± 0.06	1.44 ± 0.11
2-Butanol	0.56 ± 0.06	1.81 ± 0.15
n-Heptane	0.65 ± 0.06	1.39 ± 0.15
n-Dodecane	0.55 ± 0.20	1.25 ± 0.2
n-Hexadecane	0.55 ± 0.20	1.4 ± 0.2

For convenience the decay constants observed in all seven solvents are summarized in Table I.

E. Temperature dependence of the excited state decay

The excited state properties of DHC were explored further by measuring the lifetime as a function of temperature in a number of solvents—the two alkanes, heptane and hexadecane, and the range of alcohols: methanol, ethanol, 1-propanol, 1-butanol, and 2-butanol. The temperature was varied from 1 to 97 °C with the limits for any given sample determined by the solvent properties. Traces at the extreme temperatures in heptane, hexadecane, ethanol, and 2-butanol are shown in Fig. 11. These data illustrate a clear temperature dependence to the excited state lifetime. The transient absorption traces were fit to a biexponential decay of the excited state absorption to analyze the change in decay rate as a function of temperature. None of the solvents exhibit any significant temperature dependence to the ratio of the amplitudes of the fast and slow components.

The excited state lifetime in all solvents investigated here depends weakly on specific solvent properties, whether macroscopic properties such as viscosity or polarity, or microscopic properties such as packing and hydrogen bonding. This is particularly evident in the alkane solvents. At 25 °C the viscosity ranges from 0.387 mPa s in heptane, 1.383 mPa s in dodecane, to 3.032 mPa s in hexadecane,[51] yet the observed excited state lifetimes are nearly identical. This observation is consistent with a model where conformational changes in the initial ring-opening process are small. The solvent dependence of the rate constant in alcohols is more pronounced and the temperature dependence of these rate constants will be impacted by the temperature dependence of solvent properties including solvent viscosity. The influence of solvent must be taken into account when interpreting the data.

Analysis of the temperature dependence using the Arrhenius expression for the excited state decay constant provides an estimate for the excited state barrier including both intrinsic and solvent dependent contributions. The rate constant is given by

$$k_{obs}(T) = A_h e^{-E_a/k_B T}, \quad (4)$$

where E_a is the activation energy for internal conversion to the ground state and A_h is the frequency prefactor. The

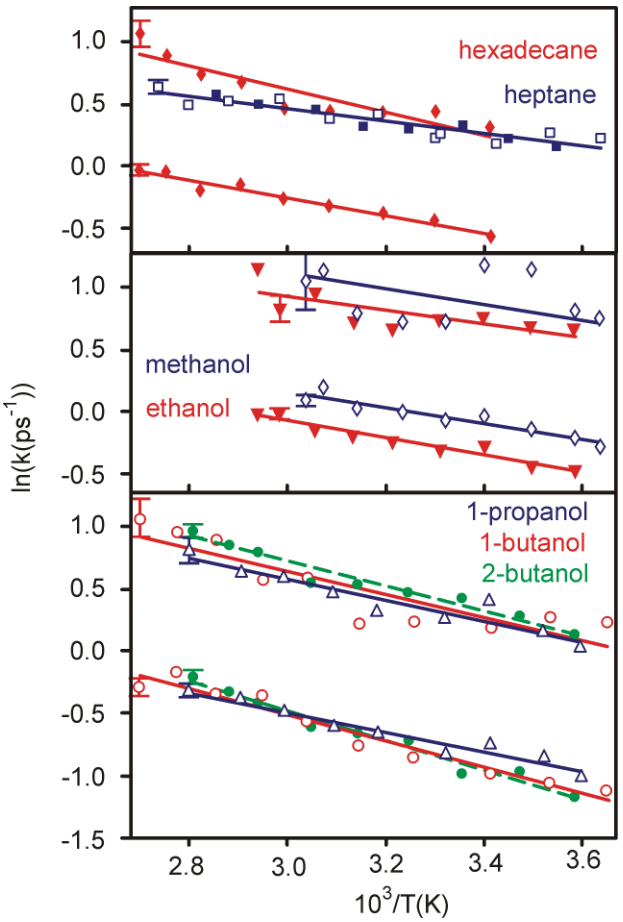

FIG. 12. Arrhenius plot of temperature dependent rate constants for the decay of the DHC ESA. Lowest panel: 2-butanol (green filled circles, 480 nm), 1-butanol (red open circles), 1-propanol (blue open triangles). Middle panel: ethanol (red filled triangles), methanol (blue open diamonds). Top panel: n-heptane (blue squares, open 500 nm, filled 620 nm), hexadecane (red filled diamonds). For n-heptane only the fast component is plotted. Typical error bars are shown for a data point in each solvent. The linear fits to the data are also shown.

relationship between $\ln(k_{obs})$ and 1/T is linear and both a barrier and prefactor can be determined for each solvent as illustrated in Fig. 12.

The fast and slow components in each solvent are approximately parallel. The barriers and Arrhenius prefactors obtained from the fits are given in Table II. The major difference is in the prefactor, not the barrier. The effective barriers and prefactors in the longer alcohols, especially in 2-butanol, are comparable to those measured for ergosterol in a low temperature 1:1 methylcyclohexane—isopropane matrix (11.1 ± 0.15 kJ/mol and 40 ± 20 ps^{-1}).[35] Separating solvent induced barriers from intrinsic intramolecular barriers is complicated. The full discussion in Sec. IV D suggests the existence of a small barrier intrinsic to the molecule as well as an extrinsic solvent dependent barrier.

F. Summary of results

The transient absorption and fluorescence experiments described above lead to a number of observations. These must be synthesized to provide a consistent view of the dynamics and reactivity of DHC in the excited electronic state(s) populated by the 266 nm laser pulse.

1. The excited state absorption spectrum is strong, broad, and relatively structureless spanning the visible from 400 to 800 nm.
2. The fluorescence spectrum and quantum yield are consistent with emission from the electronically allowed state responsible for the steady state absorption spectrum. Thus the excited state populated after 266 nm excitation is the optically allowed state.
3. The quantum yield for fluorescence is consistent with the average lifetime of the excited state population determined from the decay of the excited state absorption.
4. The decay of the excited state absorption is not single exponential, but is well modeled by a biexponential with a fast component of ~0.4–0.65 ps and a slow component 1.0–1.8 ps. These decays correspond to a biexponential decay of the total excited state population.
5. The spectral profile of the slow component is the same in all seven solvents investigated. The spectral profile of the fast component is similar to the slow component but redshifted by ~13 nm in alcohols and ~4 nm in alkanes with respect to the spectrum of the slow component.
6. The relative amplitudes of the fast and slow components depend on the solvent but do not depend on temperature within the error of the fits to the data.
7. The temperature dependence of the excited state lifetime suggests barriers for internal conversion of ~4–10 kJ/mol. The barriers arise from the intramolecular potential energy surface and the external influence of the surroundings on the molecule. The magnitude of the barriers and the amplitude of the prefactors are consistent with the values deduced for ergosterol at low temperature.
8. The absorption anisotropy is constant over the lifetime of the excited state. The integrated fluorescence anisotropy of DHC is 0.13 ± 0.01 in both heptane and 2-butanol solvents, implying an average angle of 42° ± 1° between the absorptive and emissive transition dipoles.

IV. DISCUSSION

There are at least two potential explanations for the biexponential decay of the ESA that originate from excited state relaxation (see Fig. 13): (i) The excited state population undergoes a sequential internal conversion E → I → P or E → (E ⇆ I) → P with an intermediate state "I" between the initially excited state "E" and the photoproduct "P." (ii) Dynamics on the initial excited state result in parallel decay pathways for an effectively homogeneous initial population of DHC: P ← E′ ← E → E″ → P′ (or P). In this model the initially excited state, E, branches between two excited state populations (E′ and E″) before formation of one or more photoproducts transparent in the visible region of the spectrum.

TABLE II. Effective activation energy and Arrhenius prefactor for the excited state decay of DHC as a function of solvent.

	Fast component		Slow component		Sequential model[c]	
Solvent	E_a(kJ/mol)	$A_h(ps^{-1})$	E_a(kJ/mol)	$A_h(ps^{-1})$	E_a(kJ/mol)	$A_h(ps^{-1})$
Methanol[a]			5.4 ± 0.7	8 ± 3		
Ethanol	4.5 ± 1.6	12 ± 8	5.8 ± 0.5	8 ± 2		
1-Propanol	7.0 ± 1.0	22 ± 8	6.6 ± 0.6	7 ± 2	6.5 ± 1.0	8.5 ± 3
1-Butanol	7.7 ± 1.5	30 ± 18	8.8 ± 0.7	14 ± 4	9.3 ± 1.0	26 ± 10
2-Butanol	8.3 ± 0.6	42 ± 10	9.9 ± 0.6	22 ± 5	10.3 ± 0.8	37 ± 10
n-Heptane[a]	4.2 ± 0.4	7 ± 1				
n-Hexadecane	7.7 ± 1.3	30 ± 15	5.9 ± 0.5[b]	7 ± 1	5.5 ± 0.8	7 ± 2

[a]The small relative amplitude of the slow component in n-heptane and the fast component in methanol leads to large error bars in the rate constant as a function of temperature. These do not yield reliable results and are not included in the table as separate fits.
[b]The error bar given for this barrier is from the least squares fit to the data, however there is a decay component arising from the solvent only signal on roughly the same time scale and this will decrease the overall accuracy of the fit and increase the effective error bar for the barrier.
[c]Barrier for internal conversion to product assuming a sequential model, $E \rightarrow (E \leftrightarrows I) \rightarrow P$. See the discussion section for details.

A. Sequential internal conversion

Ultrafast internal conversion from the initially excited S_2 1^1B state to a spectroscopically dark S_1 2^1A state is observed for 1,3-cyclohexadiene and many other simple polyene chromophores. Thus it is reasonable to ask if the biexponential decay of the excited state spectrum of DHC arises from such an internal conversion, $E \rightarrow I \rightarrow P$, where both E ($1^1B$) and I ($2^1A$) contribute to the transient aborption signal. The decrease in the amplitude of the excited state absorption is consistent with a change in oscillator strength accompanying a change in the electronic wave function from a S_2 $1^1B \rightarrow S_n$ transition to a S_1 $2^1A \rightarrow S_n$ transition. However, the absence of a change in the anisotropy correlated with the fast component casts doubt on the suggestion that ESA is observed from both states. If the ESA is due to an electronic transition involving the π orbitals of the polyene chromophore an internal conversion between the S_2 1^1B state and the S_1 2^1A state will result in a change in the direction of the transition dipole. Therefore, this version of the sequential model is very unlikely.

An alternative possibility is that the S_2 1^1B state and S_1 2^1A states are nearly isoenergetic in DHC. In this case the fast component corresponds approximately to the rapid equilibration of the two populations $E \rightarrow (E \leftrightarrows I)$ and the slow component corresponds approximately to the decay of this equilibrated population, $(E \leftrightarrows I) \rightarrow P$. A dipole-allowed S_2 $1^1B \rightarrow S_n$ transition from the initially populated S_2 1^1B state (E) along with a dipole-forbidden transition S_1 $2^1A \rightarrow S_n$ will account for both the constant anisotropy and the biexponential decay of the amplitude of the ESA. While the observed rate constants can be assigned qualitatively to equilibration and product formation, they are actually complex functions of the intrinsic rate constants for the equilibration of E and I and the rate constant for the formation of product from the intermediate state I.[37]

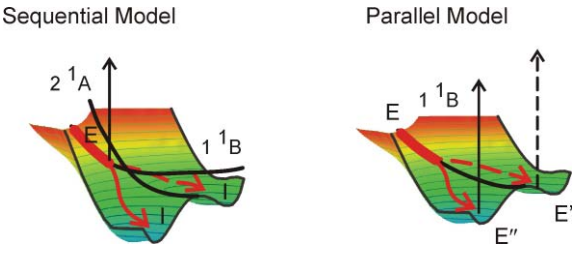

FIG. 13. Left: In a model consisting of sequential internal conversion between two excited state species, E and I, the excited state absorption probes the population "E" on the initially excited state. The decrease in intensity arises from the equilibration between E and I. The state I is drawn with two distinct minima as calculated for the isolated CHD chromophore. Right: In a model consisting of parallel excited state pathways the biexponential decay of the ESA reflects the separate decay of two excited state conformations E′ and E″.

B. Parallel model with excited state branching

A parallel model $P \leftarrow E' \leftarrow E \rightarrow E'' \rightarrow P'$ (or P), with branching of the initially excited state population (E) into two distinct populations (E′ and E″), will also account for the observed excited state decay. In this model the decay associated spectra represent the excited state spectra of the two intermediates E′ and E″ as illustrated in the right panel of Fig. 13. The amplitudes in each solvent reflect the relative populations of the two conformations.

Such a model is consistent with earlier experimental and theoretical work on the ring opening in cyclohexadiene, which may provide some insight into the ring-opening dynamics in DHC. The CHD chromophore is helical, but carries C_2 symmetry. Theoretical calculations on CHD predict that the initial motion on the optically populated 1^1B state preserves the C_2 symmetry. Distortion from the initial C_2

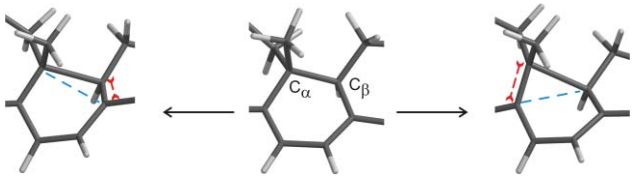

FIG. 14. Cartoon illustrating two asymmetric distortions of DHC based on the form of the symmetric distortion predicted in calculations of CHD.

symmetry provides two symmetry equivalent pathways for internal conversion from the 1^1B state to the 2^1A state; two equivalent symmetry related minima on the 2^1A state are populated prior to internal conversion to the ground state.[46–48] The gas phase studies reported by Kosma *et al.*[26] are consistent with this overall picture of the excited state motion.

The cyclohexadiene chromophore embedded in the DHC molecule is distorted from C_2 symmetry in the ground and excited states. In particular, the bonding structure around the two sp^3 carbon atoms forming the reactive C–C bond cleaved in the ring-opening reaction is different. In CHD both are CH_2 groups. In DHC one atom (C_β in Fig. 14) has three C–C bonds and a C–H bond, while the other (C_α in Fig. 14) has the C–H bond replaced by a C–CH_3 bond resulting in four C–C bonds. Thus the two alternative distortions of the cyclohexadiene chromophore are no longer equivalent. Any branching of the population on the S_2 1^1B state will be sensitive to this asymmetry. The details of the excited state potential surface will determine which distortion is preferred. The internal conversion from the S_2 1^1B state to the S_1 2^1A state and the internal conversion from the S_1 2^1A state to the ground state will also reflect the influence of this asymmetry.

C. Comparison of the sequential and parallel models

Both of the models sketched above are consistent with the general features observed in the experimental data reported above. Consideration of the evidence, however, leads to a preference for the parallel model over the sequential model. A comparison of the interpretation of the experimental data in the context of these two models is considered here.

1. Fluorescence anisotropy

The low fluorescence anisotropy observed for DHC in heptane and 2-butanol suggests a very rapid, <100 fs, conformational change in the excited electronic state following excitation. The absorption anisotropy provides some evidence for a reorientation on time scales faster than ~100 fs, but no evidence for a rotation of the transition dipole on longer time scales (Fig. 4). The rapid conformational change is consistent with a parallel model where ultrafast distortion of the CHD chromophore along the reactive ring-opening coordinate produces two related species. It is not consistent with a model where the initial configuration remains largely undistorted in the initially excited state as proposed for the sequential model. Future femtosecond time-resolved measurements of the excited state fluorescence will help to elucidate the excited state dynamics with direct measurements of the fluorescence anisotropy as a function of time.

2. Relative amplitudes

Other considerations also lead to a preference for the parallel model. The relative amplitude of the fast and slow components is dependent on solvent, but essentially independent of temperature within the error of the measurements. The parallel model, with ultrafast relaxation to two distinct minima, provides a straightforward explanation for the solvent dependence. The relative amplitude of the two components is controlled by partitioning of the population on the excited state PES. This partitioning can be modified by modest solvent dependent changes in the PES.

In the sequential model with $E \rightarrow (E \leftrightarrows I) \rightarrow P$, invoking only ultrafast equilibration among isoenergetic levels, the relative amplitude of the fast and slow components is determined by the ratio of the degeneracy or density of states in the dark state, I, to the initial excited state, E. Analysis of the data in the alcohols according to this model leads to a ratio of ~3.7 ± 0.4, with the effective degeneracy of the state I greater than that of the initially excited state E. The fluorescence quantum yield in a cryogenic glass also leads to a projected ratio of ~4 for the density of states of I/E. In the alkanes, however, the effective ratio changes with the solvent, from 13 in heptane to 7 in dodecane and 5 in hexadecane. The solvent dependence of the effective degeneracy is not easily explained by the sequential model.

3. Excited state barriers

The data presented in Fig. 12 and Table II suggest that the largest difference between the fast and slow components in the decay of DHC is in the Arrhenius prefactor A_h. In each solvent the plots of $\ln(k_{obs})$ versus 1/T are approximately parallel, but displaced. In the parallel model the two components reflect the decays of two independent excited state populations. The barrier controlling internal conversion out of the excited state manifold, ultimately repopulating the ground 1^1A ground state, will occur at a distorted asymmetric nuclear configuration. The transition state will be modified by the molecular details, including the presence or absence of the CH_3 group on C_α and C_β. Both the activation energy and the entropy of activation may be modified by molecular details. In transition state theory the rate constant, k_f, for barrier crossing is given by

$$k_f = \kappa \frac{k_b T}{h} e^{\Delta S^\dagger / k_b} e^{-\Delta H^\dagger / k_b T}, \quad (5)$$

where $\Delta S^\dagger$ is the difference in entropy between the reactant and the transition state, $\Delta H^\dagger$ is the enthalpy of activation, and κ is the Kramers coefficient accounting for the influence of the solvent on the rate.[27,30] Assuming that the influence of the solvent is similar for both channels (see below), the difference in the prefactor for the fast and slow components correlates with a difference in the entropy of activation. The two transition states for decay of the excited state will involve the C–H and C–CH_3 groups on the two sides of the active C_α–C_β bond to differing degrees, providing a mechanism for a change in the entropy of the transition state.

In the sequential model, $E \rightarrow (E \leftrightarrows I) \rightarrow P$, the temperature dependence of the observed rate constants reflects a combination of the influence of temperature on the equilibration process and on the decay of the intermediate state I. The experimental decay constants are not defined sufficiently well by the data in methanol, ethanol, or n-heptane to permit such an analysis. However, the data in the longer alcohols and hexadecane can be analyzed to extract estimates for the

intrinsic rate constants for the I → P reaction and the E → I equilibration as a function of temperature.[37] The effective barrier is strongly dependent on the solvent as shown in Table II.

The equilibration reaction E → I is also temperature dependent with effective barriers of 7.9 ± 1.0 kJ/mol in 2-butanol, 7.3 ± 2.0 kJ/mol in 1-butanol, 7.1 ± 1.4 kJ/mol in 1-propanol, and 8.0 ± 1.6 kJ/mol in hexadecane obtained from an Arrhenius plot of the intrinsic rate constants as a function of temperature. Within the error of the analysis this effective barrier is independent of the solvent. The existence of any barrier for E → I implies that a fluorescence yield approaching unity would be expected at cryogenic temperature, while a quantum yield of ~0.19 is reported at ~77 K.[35] Although the data quality and assumption of degeneracy make these barrier estimates for the equilibration reaction uncertain, this is additional support for choosing the parallel model. Further work might refine the outcome for this type of analysis.

4. Summary

In summary, both the parallel and sequential models are consistent with the transient absorption data and the fluorescence. Several factors, most significantly the low fluorescence anisotropy, lead to a preference for the parallel model. In particular, the sequential model that assigns the transient absorption to both a S_2 $1^1B \rightarrow S_n$ transition and to a S_1 $2^1A \rightarrow S_n$ transition is very unlikely. A second sequential model involving equilibration between the 1^1B and 2^1A states is considered less likely than the parallel model, but the evidence is indirect and this model cannot be ruled out. Future studies, both theoretical and experimental, will be required to fully elucidate the excited state dynamics.

D. Dependence of the excited state dynamics on the solvent

In the isolated CHD molecule internal conversion from the initially excited 1^1B state to the 2^1A state occurs on a time scale <~50 fs and internal conversion from the 2^1A state to the 1^1A ground state occurs within 100–150 fs of excitation.[26] In solution phase experiments the excited state decay occurs on comparable time scales, with the vibrationally hot ground state appearing within a few hundred femtoseconds.[28–30] The excited state dynamics are dominated by the intramolecular potential energy surface and are essentially independent of the environment.

DHC is larger than CHD and the influence of the surrounding environment cannot be ignored. The solvent dependence of the effective barrier reported in Table II points to a contribution from the environment. The influence of solvent on isomerization barriers, including the isomerization in stilbene has been studied extensively.[39,42,49] The temperature dependence of the solvent friction on the reaction coordinate provides an extrinsic barrier for the isomerization reaction in addition to the intrinsic intramolecular barrier observed for the gas phase molecule. Saltiel and co-workers[39,49] used the solvent shear viscosity and the temperature dependence of the viscosity to gain insight into the combined effects of the intrinsic and extrinsic activation barriers.

In contrast, the ground state single-bond isomerization of cZt-hexatriene → tZt-hexatriene does not exhibit any significant evidence for a viscosity dependent extrinsic barrier for isomerization.[27] Nonetheless the solvent still influences the reaction rate and the barrier in ways that depend, not on macroscopic solvent properties such as the solvent shear viscosity, but on the molecular details of the solvent. Preliminary molecular dynamics simulations suggest that the barrier for the cZt → tZt isomerization is higher in the alkanes studied by Harris *et al.* because the molecules pack tightly around the hexatriene molecule and hinder the barrier crossing. This is not observed for the more open structure of the alcohol solvents.[50]

The molecular distortion coupled to the ring-opening coordinate in DHC to form the cZc conformer of previtamin D_3 does not involve a large amplitude change in the shape of the molecule. Thus the mechanism for the influence of the solvent on the reaction coordinate must involve an indirect coupling with the solvent which affects the overall flexibility of the molecule in the excited state. Assuming that there is no static change in the intrinsic intramolecular barrier as a function of solvent, the intrinsic barrier for decay of the fast component is ≤4.2 ± 0.4 kJ/mol, with the upper limit set by the effective barriers in low viscosity ethanol and heptane solvents (Table II). The intrinsic barrier for the slow component is ≤5.4 ± 0.4 kJ/mol with the upper limit set by the effective barriers in methanol and ethanol.

The model developed by Saltiel and co-workers[39,49] provides a simple way to separate the intrinsic intramolecular and extrinsic solvent barriers for a reaction and to extract an estimate for the intrinsic barrier. The effective activation barrier is assumed to be the sum of the intrinsic barrier E_o and the barrier E_v introduced by the solvent. The solvent induced barrier can be approximated as $E_v = \alpha E_\eta$ where E_η is the activation energy for the solvent viscosity and α is a constant between 0 and 1 accounting for the fact that the relationship between reaction rate and $1/\eta$ is generally sublinear.

Using the effective activation barriers in Table II and values for E_η determined from the temperature dependence of the solvent viscosity over the range from 1 to 97 °C,[51,52] the parameters α and E_o can be estimated from the slope and intercept of a plot of E_{eff} as a function of E_η. A linear least squares fit to the data provides values of $E_o = 1.8 \pm 0.9$ kJ/mol and $\alpha = 0.30 \pm 0.05$. There may be a difference in the intrinsic barrier for the fast and slow components, but the difference is within the error estimate on E_o. These values are also consistent with the solvent dependence of the I → P transition if the data are analyzed using the sequential model for excited state decay.

While the parameters obtained from the simple model described above are reasonable, it is not clear that they accurately capture the dynamical influence of solvent on the reaction coordinate in DHC. Nakashima *et al.* reported that the fluorescence intensity for ergosterol in a methylcyclohexane:isopropanol glass was approximately constant between 77 and 89 K and decreased with increasing temperature between 89 and 150 K. The temperature dependence was used to calculate the effective barrier for the excited state decay (11.1 kJ/mol). This barrier is only slightly larger

than the effective barriers for the decay of the DHC excited state absorption in 2-butanol at room temperature (8.3 ± 0.6 kJ/mol and 9.9 ± 0.6 kJ/mol; or 10.3 ± 0.8 kJ/mole in the sequential model), although the effective viscosity is much larger. The low temperature measurement suggests that the magnitude of the solvent induced barrier saturates at ~9 kJ/mol. That is, the environment can hinder, but not prevent the ring-opening reaction. This is consistent with a mechanism where the solvent response allows molecular relaxation, lowering an intrinsic barrier for reaction within the molecule.

More detailed analysis of the excited state dynamics will require both an accurate excited state potential energy surface and a more extensive data set designed to address separately the various factors that may influence the behavior.

V. SUMMARY AND CONCLUSIONS

This study used the femtosecond time-resolved excited state absorption spectrum and time-integrated fluorescence to probe the excited state dynamics of DHC. The excited state absorption spectrum is broad and relatively structureless spanning the visible from 400 to 800 nm. There are a number of key observations in the decay of this excited state absorption that were summarized in Sec. III F. The primary observation is that the decay of the excited state absorption is not single exponential, but is well modeled by a biexponential decay with a fast component of ~0.4–0.65 ps and a slow component 1.0–1.8 ps depending on the solvent.

The temperature dependence of the excited state decay as a function of solvent suggests that there is an intrinsic intramolecular barrier to ring opening as well as a solvent dependent barrier arising from the friction of the environment on the reaction coordinate. The effective barrier in the low viscosity solvents sets an upper limit for the intrinsic barrier of ~4 kJ/mol. A simple model for the influence of the solvent provides an estimate for the intrinsic barrier of 1.8 ± 0.9 kJ/mol.

We have considered several explanations for these observations in the discussion. The preferred explanation is an ultrafast molecular distortion (<0.1 ps) on the initial 1^1B excited state that branches into two distinct minima on the 1^1B state surface. The transient spectrum probes these two configurations, which have similar excited state absorption spectra but different lifetimes for decay to either the ground state or a dark 2^1A state (as has been observed for CHD isomerization).

These new insights into the excited state of DHC suggest that coherent optical control of excited state dynamics in DHC might be possible, with potential for control of the ring-opening reaction of DHC to form previtamin D. Future work will explore the use of optical pulse shaping in both the initial excitation and excited state absorption to influence the excited state dynamics in DHC.

ACKNOWLEDGMENTS

This work has been supported by the National Science Foundation through Grants No. CHE-0718219 and through the FOCUS Center at the University of Michigan. We thank Chris Anderson and Ken Fletcher for their assistance in measuring the excited state lifetime and anisotropy decay for *trans*-stilbene in heptane and 2-butanol.

[1] A. M. Virshup, C. Punwong, T. V. Pogorelov, B. A. Lindquist, C. Ko, and T. J. Martinez, J. Phys. Chem. B **113**, 3280 (2009).
[2] V. Sundstrom, Ann. Rev. Phys. Chem. **59**, 53 (2008).
[3] E. Ritter, P. Przybylski, B. Brzezinski, and F. Bartl, Curr. Org. Chem. **13**, 241 (2009).
[4] N. A. Anderson and R. J. Sension, in *Liquid Dynamics: Experiment, Simulation, and Theory*, edited by J. T. Fourkas (American Chemical Society, Washington, D.C., 2002), Vol. 820, pp. 148–158.
[5] N. A. Anderson, J. J. Shiang, and R. J. Sension, J. Phys. Chem. A **103**, 10730 (1999).
[6] W. Fuss and S. Lochbrunner, J. Photochem. Photobiol. A **105**, 159 (1997).
[7] W. Fuss, T. Hofer, P. Hering, K. L. Kompa, S. Lochbrunner, T. Schikarski, and W. E. Schmid, J. Phys. Chem. **100**, 921 (1996).
[8] M. Kotur, T. Weinacht, B. J. Pearson, and S. Matsika, J. Chem. Phys. **130**, 134311 (2009).
[9] M. Greenfield, S. D. McGrane, and D. S. Moore, J. Phys. Chem. A **113**, 2333 (2009).
[10] E. C. Carroll, J. L. White, A. C. Florean, P. H. Bucksbaum, and R. J. Sension, J. Phys. Chem. A **112**, 6811 (2008).
[11] D. Geppert and R. de Vivie-Riedle, J. Photochem. Photobiol. A **180**, 282 (2006).
[12] D. Geppert and R. de Vivie-Riedle, Chem. Phys. Lett. **404**, 289 (2005).
[13] M. Abe, Y. Ohtsuki, Y. Fujimura, and W. Domcke, J. Chem. Phys. **123**, 144508 (2005).
[14] V. I. Prokhorenko, A. M. Nagy, S. A. Waschuk, L. S. Brown, R. R. Birge, and R. J. D. Miller, Science **313**, 1257 (2006).
[15] D. Geppert, L. Seyfarth, and R. de Vivie-Riedle, Appl. Phys. B **79**, 987 (2004).
[16] E. C. Carroll, B. J. Pearson, A. C. Florean, P. H. Bucksbaum, and R. J. Sension, J. Chem. Phys. **124**, 114506 (2006).
[17] A. C. Florean, D. Cardoza, J. L. White, J. K. Lanyi, R. J. Sension, and P. H. Bucksbaum, Proc. Natl. Acad. Sci. U.S.A. **106**, 10896 (2009).
[18] W. G. Dauben, P. E. Share, and R. R. Ollmann, J. Am. Chem. Soc. **110**, 2548 (1988).
[19] E. Havinga, R. J. Dekock, and M. P. Rappoldt, Tetrahedron **11**, 276 (1960).
[20] I. P. Terenetskaya, Theor. Exp. Chem. **44**, 286 (2008).
[21] W. G. Dauben, B. L. Zhou, and J. Y. L. Lam, J. Org. Chem. **62**, 9005 (1997).
[22] M. Braun, W. Fuss, K. L. Kompa, and J. Wolfrum, J. Photochem. Photobiol. A **61**, 15 (1991).
[23] H. J. C. Jacobs, Pure Appl. Chem. **67**, 63 (1995).
[24] O. G. Dmitrenko, I. P. Terenetskaya, and W. Reischl, J. Photochem. Photobiol. A **104**, 113 (1997).
[25] O. Dmitrenko and W. Reischl, J. Mol. Struct.: THEOCHEM **431**, 229 (1998).
[26] K. Kosma, S. A. Trushin, W. Fuss, and W. E. Schmid, Phys. Chem. Chem. Phys. **11**, 172 (2009).
[27] D. A. Harris, M. B. Orozco, and R. J. Sension, J. Phys. Chem. A **110**, 9325 (2006).
[28] S. H. Pullen, N. A. Anderson, L. A. Walker, and R. J. Sension, J. Chem. Phys. **108**, 556 (1998).
[29] S. Lochbrunner, W. Fuss, W. E. Schmid, and K. L. Kompa, J. Phys. Chem. A **102**, 9334 (1998).
[30] N. A. Anderson, S. H. Pullen, L. A. Walker, J. J. Shiang, and R. J. Sension, J. Phys. Chem. A **102**, 10588 (1998).
[31] S. Pullen, L. A. Walker, B. Donovan, and R. J. Sension, Chem. Phys. Lett. **242**, 415 (1995).
[32] W. Fuss, T. Schikarski, W. E. Schmid, S. Trushin, and K. L. Kompa, Chem. Phys. Lett. **262**, 675 (1996).
[33] W. Fuss, W. E. Schmid, and S. A. Trushin, J. Chem. Phys. **112**, 8347 (2000).
[34] N. Kuthirummal, F. M. Rudakov, C. L. Evans, and P. M. Weber, J. Chem. Phys. **125**, 133307 (2006).
[35] N. Nakashima, S. R. Meech, A. R. Auty, A. C. Jones, and D. Phillips, J. Photochem. **30**, 207 (1985).
[36] J. B. Birks and D. J. Dyson, Proc. R. Soc. London, Ser. A **275**, 135 (1963).

[37]See supplementary material at http://dx.doi.org/10.1063/1.3557054 for plots of the transient absorption signal obtained with solvent only in the sample region, comparison of this signal with the signals for DHC samples, a discussion of the nature of the excited states, S_n, responsible for the excited state absorption, and the expressions for the rate constants and amplitudes in the sequential model.
[38]G. R. Fleming, *Chemical Applications of Ultrafast Spectroscopy* (Oxford University Press, New York, 1986).
[39]J. Saltiel and Y. P. Sun, J. Phys. Chem. **93**, 6246 (1989).
[40]M. Lee, A. J. Bain, P. J. McCarthy, C. H. Han, J. N. Haseltine, A. B. Smith, and R. M. Hochstrasser, J. Chem. Phys. **85**, 4341 (1986).
[41]M. Y. Lee, J. N. Haseltine, A. B. Smith, and R. M. Hochstrasser, J. Am. Chem. Soc. **111**, 5044 (1989).
[42]J. Saltiel, A. S. Waller, D. F. Sears, and C. Z. Garrett, J. Phys. Chem. **97**, 2516 (1993).
[43]S. J. Strickler and R. A. Berg, J. Chem. Phys. **37**, 814 (1962).
[44]M. Lorenc, M. Ziolek, R. Naskrecki, J. Karolczak, J. Kubicki, and A. Maciejewski, Appl. Phys. B **74**, 19 (2002).
[45]S. A. Kovalenko, A. L. Dobryakov, J. Ruthmann, and N. P. Ernsting, Phys. Rev. A **59**, 2369 (1999).
[46]T. Mori and S. Kato, Chem. Phys. Lett. **476**, 97 (2009).
[47]H. Tamura, S. Nanbu, T. Ishida, and H. Nakamura, J. Chem. Phys. **124**, 084313 (2006).
[48]H. Tamura, S. Nanbu, H. Nakamura, and T. Ishida, Chem. Phys. Lett. **401**, 487 (2005).
[49]J. Saltiel and J. T. D'Agostino, J. Am. Chem. Soc. **94**, 6445 (1972).
[50]F. X. Vazquez, Ph.D. dissertation, University of Michigan, 2010.
[51]"Viscosity of liquids," in *CRC Handbook of Chemistry and Physics*, 91st ed., internet version 2011, edited by W. M. Haynes (CRC Press/Taylor and Francis, Boca Raton, FL).
[52]C. Yang, Y. Sun, Y. He, and P. Ma, J. Chem. Eng. Data **53**, 293 (2008).